View metadata, citation and similar papers at core.ac.uk

brought to you by CORE

provided by Elsevier - Publisher Connector

Ain Shams Engineering Journal (2014) 5, 1277–1286

Ain Shams University

Ain Shams Engineering Journal

www.elsevier.com/locate/asej
www.sciencedirect.com

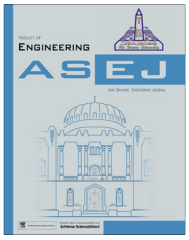

ENGINEERING PHYSICS AND MATHEMATICS

Effect of radiation on transient MHD flow of micropolar fluid between porous vertical channel with boundary conditions of the third kind

D. Prakash, M. Muthtamilselvan *

Department of Applied Mathematics, Bharathiar University, Coimbatore 641 046, India

Received 20 January 2014; revised 10 April 2014; accepted 10 May 2014
Available online 20 June 2014

KEYWORDS

MHD;
Micropolar fluid;
Thermal radiation;
Fully developed flow

Abstract The present work is devoted to investigate the effect of thermal radiation on fully developed flow of micropolar fluid flowing between the two infinite parallel porous vertical plates in the presence of transverse magnetic field. The fluid is considered to be a gray, absorbing–emitting but non-scattering medium, and the Cogley–Vincent–Gilles formulation is adopted to simulate the radiation component of heat transfer. The rigid plates are assumed to exchange the heat with an external fluid by convection. The governing equations are solved numerically by Crank–Nicolson implicit finite difference method. The effect of various physical parameters such as transient, Hartmann number, micropolar parameter, radiation parameter, Prandtl number, Biot number and Reynolds number on the velocity and temperature field are discussed graphically. The important finding of the present work is that the temperature of the fluid is reduced by applying thermal radiation. Further, the results obtained under the limiting conditions were found to be in good agreement with the existing one.

© 2014 Production and hosting by Elsevier B.V. on behalf of Ain Shams University.

1. Introduction

In the most of the analyses on the flow and heat transfer in a channel, either the boundary condition of the first kind characterized by the prescribed wall temperature or the boundary condition of the second kind expressed by the prescribed wall heat flux is assumed. A more realistic condition in many applications, however, will be the temperature boundary condition of the third kind: the local wall heat flux is a linear function of the local wall temperature. This situation is relatively less studied and is encountered in the heat transfer process, where the radiative heat transfer, describable in terms of Newton's law of cooling, occurs at the channel wall [1]. Considering of its importance, several authors [2–4] have investigated the problem with the boundary condition of the third kind.

Analysis of the flow and heat transfer of micropolar fluid in a vertical channel has been of great interest because the Navier–Stokes equations for Newtonian fluids cannot successfully describe the characteristics of fluid with suspended particles. Unlike the other fluids, micropolar fluids may be described as non-Newtonian fluids consisting of dumb-bell molecules or

* Corresponding author. Tel.: +91 422 2422222.
E-mail address: muthtamill@yahoo.co.in (M. Muthtamilselvan).

Peer review under responsibility of Ain Shams University.

ELSEVIER Production and hosting by Elsevier

2090-4479 © 2014 Production and hosting by Elsevier B.V. on behalf of Ain Shams University.
http://dx.doi.org/10.1016/j.asej.2014.05.004

Nomenclature

B, C	micropolar material constants
c_p	specific heat, J kg^{-1} K^{-1}
g	acceleration due to gravity, m s^{-2}
j	micro-inertia density, m^2
H_0	magnetic field intensity, W e m^{-2}
h_1	external convection coefficient at the left wall, W m^{-2} K^{-1}
h_2	external convection coefficient at the right wall, W m^{-2} K^{-1}
k	thermal conductivity, W m^{-1} K^{-1}
K	rotational viscosity coefficient, kg s^{-1} m^{-1}
L	thickness of the channel, m
M	Hartmann number
N	dimensionless angular velocity
n	angular velocity, rad s^{-1}
N_R	dimensionless thermal radiation parameter
Pr	Prandtl number
q_r	radiative heat flux
Re	cross flow Reynolds number
T	temperature, K
T_0	temperature in hydrostatic state, K
v_0	suction/injection velocity, m s^{-1}
u, v	velocities in x, y-directions, m s^{-1}
x, y	axial and perpendicular co-ordinates, m
Y	dimensionless co-ordinate

Greek symbols

β	volumetric coefficient of thermal expansion, K^{-1}
γ	microrotational coupling coefficient, N s
ν	kinematic viscosity, m^2 s^{-1}
ρ	density, kg m^{-3}
σ	electrical conductivity, Ω^{-1} m^{-1}
τ	dimensionless time
θ	dimensionless temperature
λ_1	micropolar parameter
λ_2	micropolar material constant

Subscripts

i, j	nodes along Y, τ directions respectively
N	end boundary node along Y direction
w	condition at the wall

short rigid cylindrical element, polymer fluids, fluid suspension, etc. In addition with the classical velocity field, a microrotation vector and a gyration parameter are introduced in the micropolar fluid model in order to investigate the kinematics of microrotation. The theory of micropolar fluids, first proposed by Eringen [5,6], can be used to study the behaviors of exotic lubricants, polymeric suspensions, muddy and biological fluids, animal blood, colloidal solutions, liquid crystals with rigid molecules, etc. The presence of dust or smoke, in particular in a gas may also be modeled using micropolar fluid dynamics. A comprehensive reviews of the theory and applications can be found in the review articles by Ariman et al. [7,8] and the recent books by Lukaszewicz [9] and Eringen [10].

The problem of fully developed flow in a micropolar fluid is discussed by Balaram and Sastry [11]. Agarwal and Dhanapal [12] obtained a numerical solution to study the fully developed free convective flow between two parallel walls with suction (or injection) embedded in a micropolar fluid. Chamkha et al. [13] analyzed the fully developed free convective flow of a micropolar fluid in vertical parallel plate channel with asymmetric heating by numerically and analytically. The closed-form analytic solutions for the flow and heat transfer characteristics of micropolar fluid in a vertical channel are given by Cheng [14]. Prathap kumar et al. [15] studied the problem of fully developed free convective flow in a vertical channel, partially filled with micropolar fluid. The effect of heat source/sink on fully developed mixed convection flow of micropolar fluid mixture in a vertical channel with the boundary conditions of the third kind is investigated by Umavathi and Sultana [16]. They stated that the values of all the characteristics of a micropolar fluid were found to be lower than those for a Newtonian fluid. By applying Differential Transform Method (DTM) and Homotopy Analysis Method (HAM), Rashidi et al. [17–19] investigated the second grade fluid flow through porous media past a horizontal surface and rotating disk. Fully developed flow through a porous channel in the presence of heat generation is examined asymptotically by Prakash et al. [20]. Recently, Sheikholeslami et al. [21] analyzed the problem of micropolar fluid flow in a channel subject to a chemical reaction by using homotopy perturbation method.

The problem of micropolar fluids through porous media has many applications, such as porous rocks, foams and foamed solids, aerogels, alloys, polymer blends, and microemulsions. In recent years, many authors have studied unsteady free convection flow of a micropolar fluid with or without a magnetic field through a porous medium. For example, Srinivasacharya et al. [22] discussed the effects of microrotation and frequency parameters on an unsteady flow of micropolar fluid between two parallel porous plates with a periodic suction. Bhargara et al. [23] obtained a numerical solution of a free convection MHD micropolar fluid flow between two parallel porous vertical plates by means of the quasi-linearization method. Zueco et al. [24] investigated the transient hydromagnetic flow of micropolar fluid between parallel porous vertical walls using Network Simulation Method. They concluded that the magnetic field should be important parameter for controlling the rate of heat transfer in many MHD applications.

At high temperature, thermal radiation can be significantly affect the heat transfer and the temperature distribution of a micropolar fluid in a channel. Heat transfer by simultaneous free convection and thermal radiation in the case of a micropolar fluid has not gained as much attention. This is unfortunate because thermal radiation plays an important role in determining the overall surface heat transfer in situations where convective heat transfer coefficients are small, as is the case in free convection where such situations are common in space technology [25]. Radiation effects on a micropolar fluid through a porous medium with and without magnetic field has been considered by many authors, see [26–29].

In this analysis, we study the effect of thermal radiation on a transient electrically conducting micropolar fluid in between two porous vertical plates submitted to an external magnetic field. The plates exchange heat with an external fluid, and both conditions of equal and different reference temperatures of the external fluid are considered. Crank–Nicolson implicit finite difference (C–N) method is used to solve the governing equations.

2. Mathematical formulation

Consider an unsteady, laminar, fully developed free convective flow of an incompressible micropolar fluid flowing between two infinite parallel porous vertical plates submitted to a strong magnetic field H_0 in the direction normal to the plate. Since the magnetic Reynolds number is assumed to be small enough, the induced magnetic field can be neglected. The micropolar fluid is assumed to be a gray, absorbing-emitting, but non-scattering medium. Outside the plate, there is a quiescent ambient fluid at a constant temperature T_∞ with u and v denoting, respectively, the velocity components in the x and y direction, where x is vertically upwards and y is the coordinate perpendicular to x. There is a component of microrotation in the direction normal to x and y, $(0,0,n)$. All fluid properties are considered to be constant except for the density variation which induces the buoyancy force. Neglecting the effect of viscous dissipation, the governing equations can be written as

$$\frac{\partial v}{\partial y} = 0 \tag{2.1}$$

$$\frac{\partial u}{\partial t} + v_0\left(\frac{\partial u}{\partial y}\right) = \left(\frac{\upsilon + K}{\rho}\right)\frac{\partial^2 u}{\partial y^2} + \beta g(T - T_0) + \left(\frac{K}{\rho}\right)\frac{\partial n}{\partial y} - \frac{\sigma H_0^2}{\rho}u \tag{2.2}$$

$$\rho j\left(\frac{\partial n}{\partial t}\right) + v_0\rho j\left(\frac{\partial n}{\partial y}\right) = \gamma\left(\frac{\partial^2 n}{\partial y^2}\right) - K\left(2n + \frac{\partial u}{\partial y}\right) \tag{2.3}$$

$$\rho c_p\left(\frac{\partial T}{\partial t}\right) + \rho c_p v_0\left(\frac{\partial T}{\partial y}\right) = k\left(\frac{\partial^2 T}{\partial y^2}\right) - \frac{\partial q_r}{\partial y} \tag{2.4}$$

where β is the thermal expansion co-efficient, ρ is the density, c_p is the specific heat, k is the thermal conductivity of the fluid, υ is the kinematic viscosity, K is the gyroviscosity, γ is the material constant, j the microinertia, σ the electrical conductivity of the fluid and T_0 is the temperature in hydrostatic state, with γ_0 the constant of proportionality.

The advantages and limitations of the Cogley–Vincent–Gilles [30] formulation, which is to used to simulate the radiation component of heat transfer, are

(i) it does not require an extra transport equation for the incident radiation, and
(ii) it can only be used for an optically thin, near-equilibrium and non-gray gas.

Cogley model is well suited for

(i) surface-to-surface radiant heating or cooling,
(ii) coupled radiation, convection, and/or conduction heat transfer and
(iii) radiation in glass processing, glass fiber drawing, and ceramic processing.

Following Cogley et al. [30], we take the expression of radiative heat flux as

$$\frac{\partial q_r}{\partial y} = 4(T - T_0)\int_0^\infty K_{\lambda h}\left(\frac{\partial e_{\lambda p}}{\partial T}\right)_L d\lambda \tag{2.5}$$

where $K_{\lambda h}$ is the absorption coefficient, λ is the wave length, $e_{\lambda p}$ is the Planck's function, T is the temperature of the walls at time $t \leqslant 0$.

On the use of Eq. (2.5), Eq. (2.4) becomes,

$$\rho c_p\frac{\partial T}{\partial t} + \rho c_p v_0\left(\frac{\partial T}{\partial y}\right) = k\frac{\partial^2 T}{\partial y^2} - 4(T - T_0)I \tag{2.6}$$

where

$$I = \int_0^\infty K_{\lambda h}\left(\frac{\partial e_{\lambda p}}{\partial T}\right)_L d\lambda \tag{2.7}$$

Both walls of the channel are assumed to have a negligible thickness and to exchange heat with an external fluid by convection. At $y = 0$, the external convection coefficient h_1 is considered uniform and the fluid in the region $y < 0$ is assumed to have a uniform reference temperature T_1. At $y = L$, the corresponding constant values are h_2 and T_0 $(T_0 \geqslant T_1)$. With the assumption of zero spin at the fluid–solid interface, the initial and boundary conditions are written as follows:

$$\text{for } t \leqslant 0; \quad u = 0, \quad n = 0, \quad T = T_0 \tag{2.8}$$

$$\text{for } t > 0; \quad u = 0, \quad v = v_0, \quad n = 0,$$

$$-k_w\frac{\partial T}{\partial y} = h_1[T_1 - T] \quad \text{at} \quad y = 0 \tag{2.9}$$

$$u = 0, \quad v = v_0, \quad n = 0,$$

$$-k_w\frac{\partial T}{\partial y} = h_2[T - T_0] \quad \text{at} \quad y = L \tag{2.10}$$

where v_0 is the constant suction or injection of the fluid through the porous limiting surface, with $v_0 < 0$ implies injection at $y = L$ and suction at $y = 0$, while the opposite occurs for $v_0 > 0$. In order to dimensionalize the governing equations, we introduce the following dimensionless variables

$$\left.\begin{aligned} &Y = \frac{y}{L}, \quad U = \frac{u\rho g\beta L^2}{k}, \quad \tau = \frac{tu}{L^2}, \quad \theta = \frac{(T - T_0)\rho^2 g^2\beta^2 L^4}{k\mu}, \\ &N = \frac{n\rho g\beta L^2\upsilon n}{k}, \quad Pr = \frac{\upsilon}{\alpha}, \quad M^2 = \frac{\sigma H_0^2}{\mu}, \quad Re = \frac{v_0\rho L}{\mu}, \\ &\lambda_1 = \frac{K}{\mu}, \quad \lambda_2 = \frac{\gamma}{\mu L^2}, \quad B = \frac{j}{L^2}, \quad C = \frac{L^2}{1 + \lambda_1} \end{aligned}\right\} \tag{2.11}$$

where M^2 is the Hartmann number, λ_1 is the micropolar parameter, γ_0 is the dimensionless of heat generated, λ_2, B and C are the micropolar material constants and Re is the cross flow Reynolds number.

With the help of Eq. (2.11), the governing equations can be rewritten in the form

$$\left(\frac{\partial U}{\partial \tau}\right) + Re\left(\frac{\partial U}{\partial Y}\right) = (1 + \lambda_1)\left(\frac{\partial^2 U}{\partial Y^2}\right) + \theta + \lambda_1\left(\frac{\partial N}{\partial Y}\right) - CM^2 U \tag{2.12}$$

$$B\left(\frac{\partial N}{\partial \tau}\right)+ReB\left(\frac{\partial N}{\partial Y}\right)=\lambda_2\left(\frac{\partial^2 N}{\partial Y^2}\right)-\lambda_1\left(\frac{\partial U}{\partial Y}+2N\right) \quad (2.13)$$

$$Pr\left(\frac{\partial \theta}{\partial \tau}\right)+RePr\left(\frac{\partial \theta}{\partial y}\right)=\left(\frac{\partial^2 \theta}{\partial Y^2}\right)-N_R\theta \quad (2.14)$$

and the dimensionless initial and boundary conditions become,

$$\tau \leqslant 0: \quad U=0; \quad N=0; \quad \theta=0 \quad (2.15)$$

$$\tau>0: \quad U=0; \quad N=0; \quad -\frac{\partial \theta}{\partial Y}=Bi_1[\xi-\theta] \quad \text{at} \quad Y=0 \quad (2.16)$$

$$\tau>0: \quad U=0; \quad N=0; \quad -\frac{\partial \theta}{\partial Y}=Bi_2[\theta-\epsilon\xi] \quad \text{at} \quad Y=1 \quad (2.17)$$

where $\xi=\frac{PrGr\beta gL}{c_p}$ is a dimensionless group, $Gr=\frac{\beta gL^3(T-T_0)}{\nu^2}$ is a Grashof number, $\epsilon=\frac{T_2-T_0}{T_1-T_0}$ is a nondimensional heating parameter, $Bi_1=\frac{h_1}{k_w}$, $Bi_2=\frac{h_2L}{k_w}$ are the Biot numbers, k_w is the thermal conductivity of the walls and $N_R=\frac{4IL^2}{k}$ is the thermal radiation parameter.

The shear, couple stresses and the heat flux on the walls are defined, respectively, as

$$\tau_w=(\mu+K)\left.\frac{\partial u}{\partial y}\right|_{y=0,1}, \quad \tau_m=\gamma\left.\frac{\partial n}{\partial y}\right|_{y=0,1} \quad \text{and} \quad q_w=-k\left.\frac{\partial T}{\partial y}\right|_{y=0,1} \quad (2.18)$$

3. Numerical procedure

For solving the governing Eqs. (2.12)–(2.14) subject to the initial and boundary conditions given by (2.15)–(2.17), Crank–Nicolson implicit finite difference technique has been employed. The computational domain $(0<\tau<\infty)$ and $(0<Y<1)$ is divided into a mesh of lines parallel to τ and Y axes. The finite difference approximations of Eqs. (2.12)–(2.17) are obtained by substituting the approximations by derivatives. Thus, the governing equations and boundary conditions are transformed into the following algebraic equations:

$$\left(\frac{U_{i,j+1}-U_{i,j}}{\Delta\tau}\right)+Re\left(\frac{U_{i+1,j}-U_{i,j}}{\Delta Y}\right)=(1+\lambda_1)\left(\frac{U_{i-1,j}-2U_{i,j}+U_{i+1,j}}{(\Delta Y)^2}\right)+\theta_{i,j}+\lambda_1\left(\frac{N_{i+1,j}-N_{i,j}}{\Delta Y}\right)-CM^2U_{i,j} \quad (3.1)$$

$$B\left(\frac{N_{i,j+1}-N_{i,j}}{\Delta\tau}\right)+ReB\left(\frac{N_{i+1,j}-N_{i,j}}{\Delta Y}\right)=\lambda_2\left(\frac{N_{i-1,j}-2N_{i,j}+N_{i+1,j}}{(\Delta Y)^2}\right)-\lambda_1\left(\frac{U_{i+1,j}-U_{i,j}}{\Delta Y}+2N_{i,j}\right) \quad (3.2)$$

$$Pr\left(\frac{\theta_{i,j-1}-\theta_{i,j}}{\Delta\tau}\right)+RePr\left(\frac{\theta_{i+1,j}-\theta_{i,j}}{\Delta Y}\right)=\left(\frac{\theta_{i-1,j}-2\theta_{i,j}+\theta_{i+1,j}}{(\Delta Y)^2}\right)-N_R\theta_{i,j} \quad (3.3)$$

and the associated initial and boundary conditions may be expressed as

$$U_{i,1}=0; \quad N_{i,1}=0; \quad \theta_{i,1}=0 \quad (3.4)$$

$$U_{1,j}=0; \quad N_{1,j}=0, \quad -\frac{\theta_{1,j-1}-\theta_{1,j}}{\Delta Y}=Bi_1[\xi-\theta_{1,j}] \quad (3.5)$$

$$U_{N,j}=0; \quad N_{N,j}=0, \quad -\frac{\theta_{N,j-1}-\theta_{N,j}}{\Delta Y}=Bi_2[\theta_{N,j}-\epsilon\xi] \quad (3.6)$$

where ΔY and $\Delta\tau$ are the mesh sizes along Y and time directions, respectively. The computational domain $(0<\tau<\infty)$ is divided into intervals with step size $\Delta\tau=0.002$ for time (τ). In order to check the stability of finite difference scheme, computation is carried out for different grids $(0<Y<1)$, and it is seen that it does not show any significant change after the grid size 201 (see Fig. 1). Therefore, all the numerical solutions are obtained with the grid size 201. To check the numerical code, we compare our results with Zueco et al. [24]

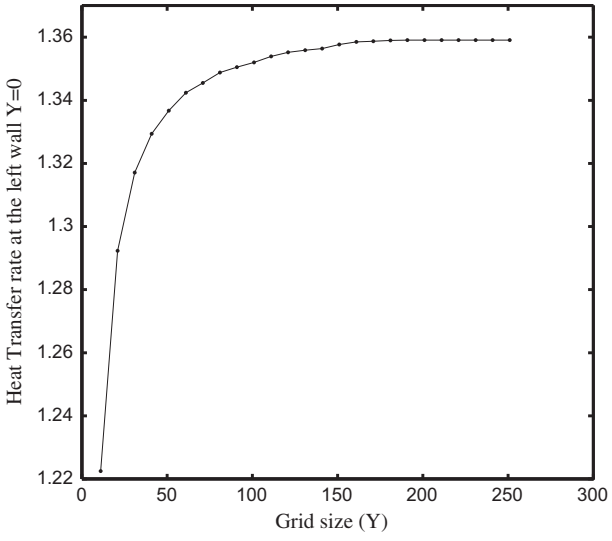

Figure 1 Heat transfer rate at the left wall $Y=0$ for different grid systems with $\tau=0.2$, $Re=-2$, $\lambda_1=3$, $M^2=N_R=1$, $Pr=0.72$, $Bi_1=10$, $Bi_2=1$.

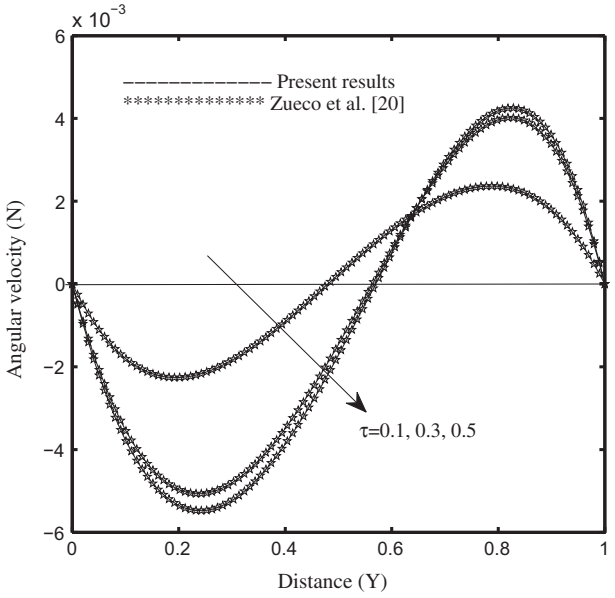

Figure 2 Comparison of results with Zueco et al. [24] for $Re = 5,\ \lambda_1 = 3,\ M^2 = 10,\ Pr = 0.73,\ Bi_1 = 10,\ Bi_2 = 1$.

through graphically and it is presented in Fig. 2. It is seen that the present numerical results are in good agreement with Zueco et al. [24].

4. Results and discussion

The results are presented for a range of values of the non-dimensional parameters such as cross flow Reynolds number Re, Hartmann number M^2, micropolar parameter λ_1, Prandtl number Pr, thermal radiation parameter N_R and Biot numbers Bi_1 and Bi_2. The values of the parameters $Bi_1 = 10,\ Bi_2 = 1,\ \xi = 1.0,\ \epsilon = 1.2,\ \lambda_2 = 1.0,\ B = 0.001,\ C = 1.0,\ \lambda_1 = 3.0,\ Pr = 0.72,\ Re = 2.0,\ M^2 = N_R = 1.0$ are fixed, unless otherwise specified.

4.1. Hydrodynamic aspects

Fig. 3 shows the transient $(\tau = 0.1, 0.2, 0.3)$ response to study the effect of Reynolds number on the velocity profile. It can be seen that with the fixed values of time parameter, an increase in the Reynolds number is to increase the velocity profile at the middle of the channel. Moreover, the velocity profile increases with time to reach the steady state.

The effect of Hartmann number on the stationary spatial velocity distribution for $Re = 1$ and for $Re = 10$ is shown in Fig. 4. It is observed that the velocity profiles are parabolic and reach their maximum near the middle, but this maximum is displaced toward $Y = 1$ for large Reynolds number. Besides, an increases in M^2 yield a decrease in the velocity profiles.

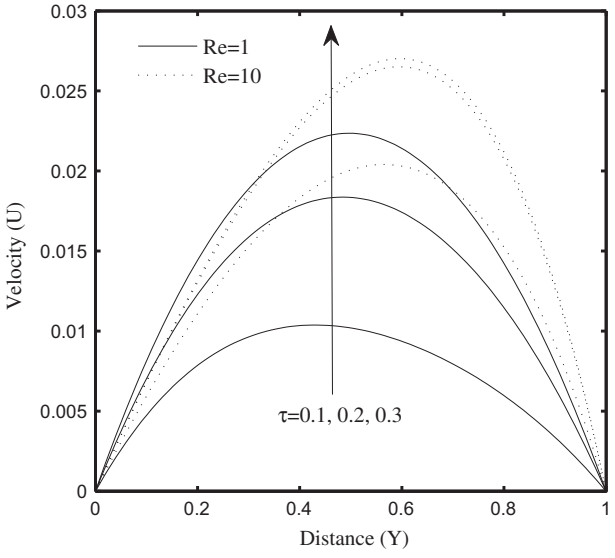

Figure 3 Dimensionless velocity profile for transient (τ) and Reynolds number (Re).

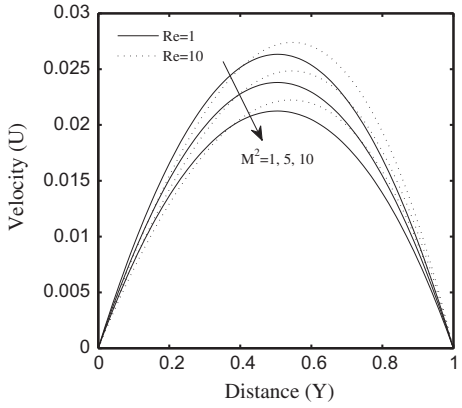

Figure 4 Dimensionless velocity profile for Hartmann number (M^2) and Reynolds number (Re).

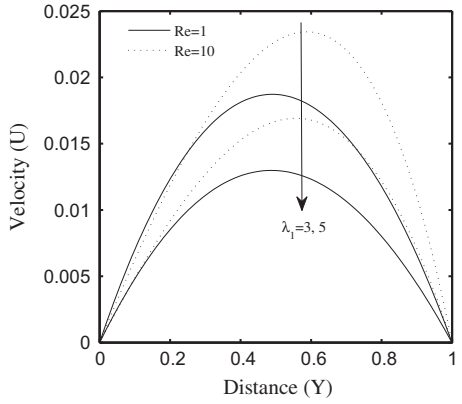

Figure 5 Dimensionless velocity profile for Micropolar parameter (λ_1) and Reynolds number (Re).

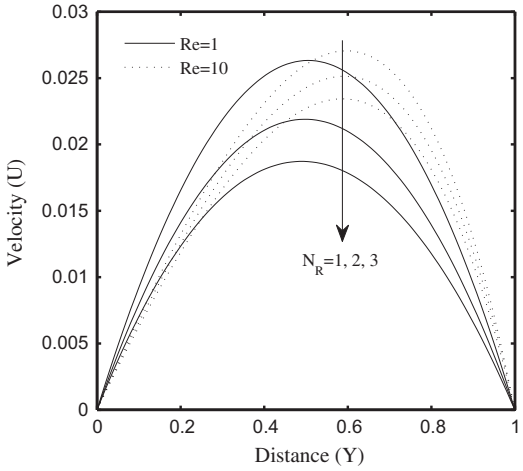

Figure 6 Dimensionless velocity profile for radiation parameter (N_R) and Reynolds number (Re).

Therefore, the fluid velocity can be reduced by the presence of a strong magnetic field. The influence of cross flow Reynolds number Re, micropolar parameter λ_1 on the velocity profile is analyzed in Fig. 5. As expected, the velocity profile increases as Re increases. It is noted that the velocity profile decreases with increase in the micropolar parameter.

Fig. 6 depicts the velocity distribution along the spatial coordinate Y for different values of radiation parameter. The velocity distribution decreases with an increase in the radiation parameter. Also the maximum velocity is displaced toward $Y = 1$ for higher Reynolds number $Re = 10$.

Fig. 7 is plotted to analyze the transient response in the angular velocity distribution. As seen from this figure, the angular velocity increases with time; the values of microrotation are negative between $Y = 0$ and $Y = 0.5$ approximately, whereas they are positive between $Y = 0.5$ and $Y = 1$ approximately; besides, as Reynolds number increases the amplitude of the angular velocity.

The effects of Hartmann number and the Reynolds number on the angular velocity profile is shown in Fig. 8. It is noted

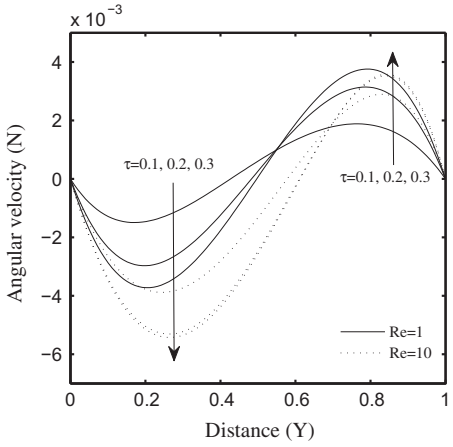

Figure 7 Dimensionless angular velocity profile for transient (τ) and Reynolds number (Re).

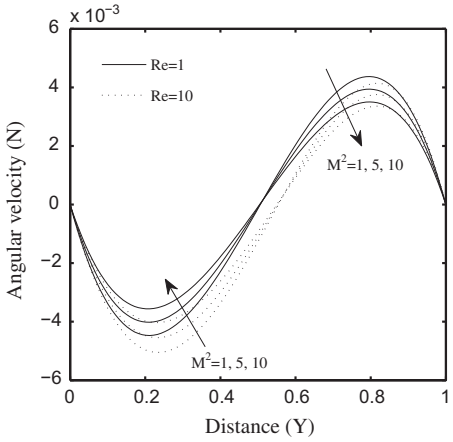

Figure 8 Dimensionless angular velocity profile for Hartmann number (M^2) and Reynolds number (Re).

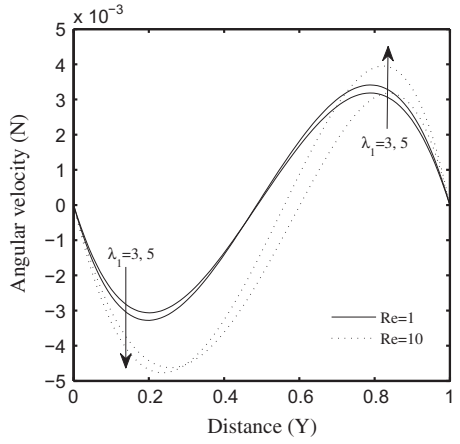

Figure 9 Dimensionless angular velocity profile for micropolar parameter (λ_1) and Reynolds number (Re).

that an increase in the Hartmann number is to increase the angular velocity between $Y = 0$ and $Y = 0.5$, whereas decrease it in between $Y = 0.5$ and $Y = 1$. But this behavior is moved toward $Y = 1$ for the case of large Reynolds number.

Fig. 9 portrays the angular velocity distribution for different values of micropolar parameter. It is seen that the micropolar parameter strongly influences the angular velocity. In the case of higher Reynolds number, the micropolar parameter enforces to increase the angular velocity almost full length of the channel.

The influence of the radiation parameter on the angular velocity profile is depicted in Fig. 10. It can be seen that the radiation effect lead to increase the angular velocity for the first half of the channel and decrease it for the remaining. Further, an increase in the Reynolds number is to decrease the angular velocity throughout the channel. Table 1 shows that an increase in the magnetic parameter is to decrease the shearing rates for the left wall, whereas increase it in the right wall.

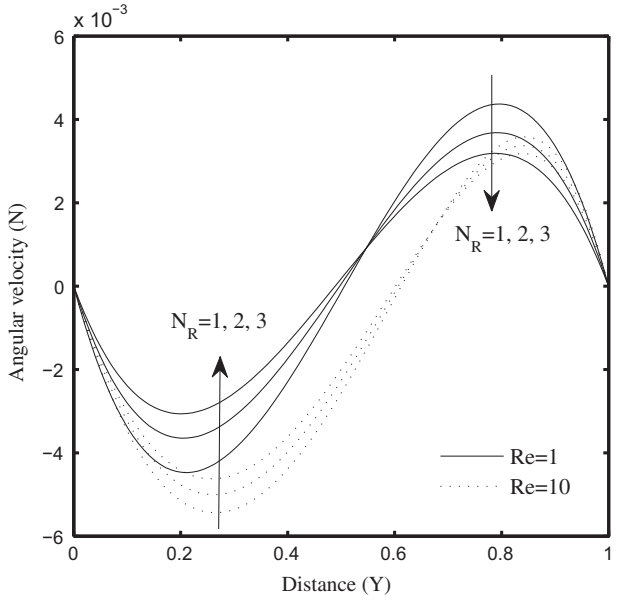

Figure 10 Dimensionless angular velocity profile for radiation parameter (N_R) and Reynolds number (Re).

Table 1 Shear and couple stresses along the plates ($\tau = 0.2, N_R = 1.0, Pr = 0.72$).

Re	λ_1	M^2	Shear and couple stresses			
			$\frac{dU}{dY}\|_{Y=0}$	$\frac{dU}{dY}\|_{Y=1}$	$\frac{dN}{dY}\|_{Y=0}$	$\frac{dN}{dY}\|_{Y=1}$
−2	3	0	0.0781	−0.0598	−0.0301	−0.0287
		1	0.0767	−0.0588	−0.0294	−0.0281
		2	0.0754	−0.0578	−0.0288	−0.0274
	5	0	0.0522	−0.0421	−0.0336	−0.0319
		1	0.0516	−0.0415	−0.0331	−0.0314
		2	0.0509	−0.0410	−0.0326	−0.0309
2	3	0	0.0811	−0.0804	−0.0358	−0.0356
		1	0.0798	−0.0787	−0.0349	−0.0348
		2	0.0785	−0.0771	−0.0342	−0.0340
	5	0	0.0566	−0.0535	−0.0398	−0.0392
		1	0.0559	−0.0527	−0.0392	−0.0385
		2	0.0552	−0.0520	−0.0385	−0.0379

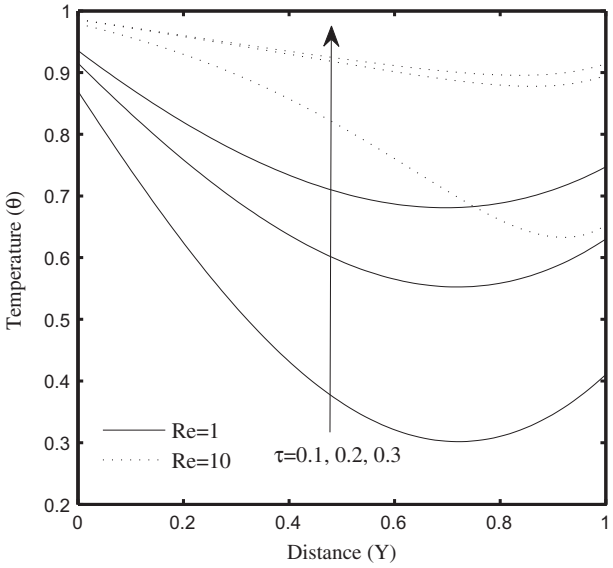

Figure 11 Dimensionless temperature distribution for transient (τ) and Reynolds number (Re).

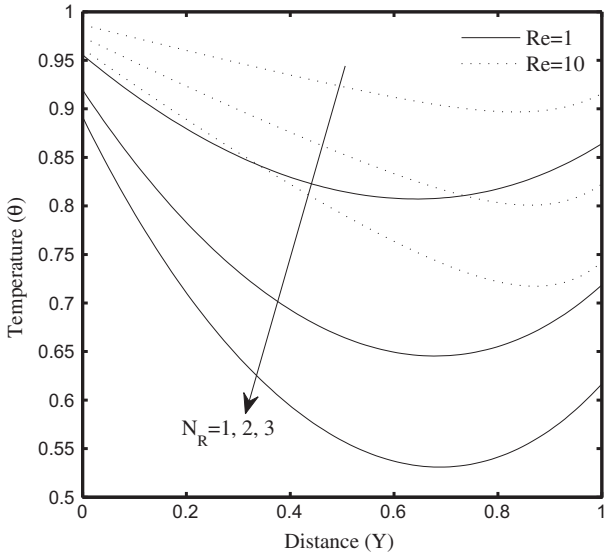

Figure 12 Dimensionless temperature distribution for radiation parameter (N_R) and Reynolds number (Re).

The reverse trend is observed in the case of Reynolds number or the micropolar parameter.

4.2. Heat transfer aspects

The temperature distribution along the spatial coordinate Y for the case of transient is shown in Fig. 11. It is observed that with the fixed values of Reynolds number, the temperature increases with time. Also, the influence of Reynolds number is to increase the fluid temperature.

The effect of radiation parameter on the temperature distribution is illustrated in Fig. 12. It is observed that an increase in the radiation parameter is to decrease the temperature due to the absorption of temperature from the fluid. Moreover, in the case of low Reynolds number, the temperature decreases up to the middle of the channel and increases after that. But this point of inflection is shifted from the middle to the right wall in the case of large Reynolds number.

Fig. 13 is presented to analyze the effect of radiation on the temperature field for the case of convection heat flux is applied in the left wall or the right wall. As already mentioned, the radiation lead to decrease the fluid temperature in both cases of convective heating. Comparing the temperature at the walls, the highest temperature is obtained at the left wall or right wall in the case of convective heat flux applied in the left wall or right wall respectively.

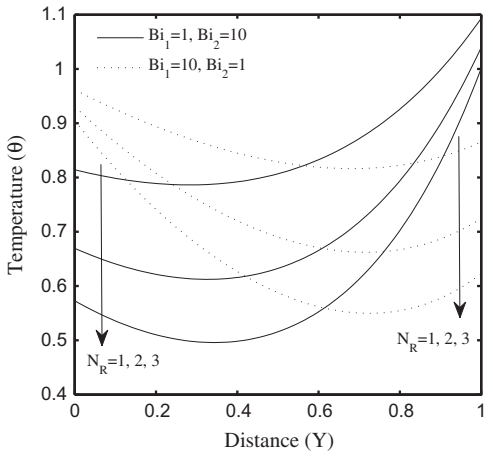

Figure 13 Dimensionless temperature distribution for radiation parameter (N_R) and Reynolds number (Re) with different type of heating.

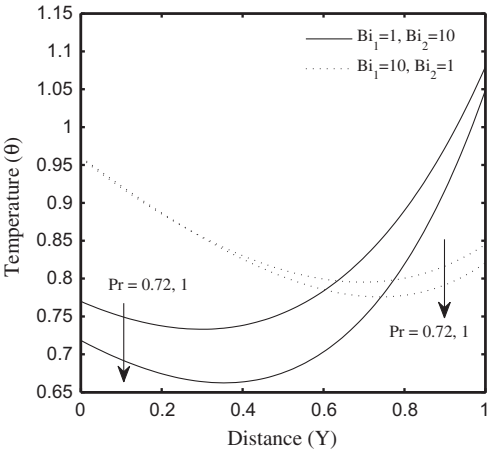

Figure 14 Dimensionless temperature distribution for Prandtl number (Pr) and Reynolds number (Re) with different type of heating.

The effect of Prandtl number on the temperature field is plotted in Fig. 14. It is observed that an increase in the Prandtl number is to decrease the temperature in the case of convective heating of the right wall; whereas in left wall heating, the fluid temperature increases near the left wall and decreases away from the left wall. Table 2 elucidates that in the case of heat flux applied to the left wall, the effect of radiation is to absorb the heat from the right wall and produce it to the left wall, while the reverse effect is seen for the case of heat flux applied to the right wall.

5. Conclusions

The effect of thermal radiation on the fully developed flow of micropolar fluid between the two vertical infinite plates in the presence of transverse magnetic field is investigated numerically by Crank–Nicolson scheme. From the present investigation the following conclusions may be drawn:

1. An increase in the Reynolds number is to increase the velocity and the temperature, but decrease the angular velocity with the fixed values of other parameters.
2. An increase in the magnetic, micropolar or radiation parameter is to decrease the velocity throughout the channel. However in the angular velocity field, the magnetic or radiation parameter is to increase the angular velocity in the first half of the channel and decrease in the remaining.
3. An increase in the radiation parameter or Prandtl number is to decrease the temperature.
4. When the heat flux is applied in the left wall or right wall, the highest temperature is observed in the corresponding walls.

Acknowledgements

The authors wish to express their sincere thanks to the honorable referees for their valuable comments to improve the quality of the paper.

Table 2 Local heat flux along the plates ($\tau = 0.2, M^2 = 1.0, \lambda_1 = 3.0$).

Re	Pr	N_R	$Bi_1 = 10,\ Bi_2 = 1$		$Bi_1 = 1,\ Bi_2 = 10$	
			$-\frac{d\theta}{dY}\|_{Y=0}$	$-\frac{d\theta}{dY}\|_{Y=1}$	$-\frac{d\theta}{dY}\|_{Y=0}$	$-\frac{d\theta}{dY}\|_{Y=1}$
−2	0.72	0	1.0952	−0.4856	0.2542	−0.5796
		1	1.3520	−0.5482	0.3362	−0.8502
		2	1.5759	−0.6012	0.4049	−1.0916
	7.0	0	5.4873	−0.7703	0.8572	−0.6425
		1	5.4954	−0.7748	0.8576	−0.6998
		2	5.5034	−0.7793	0.8580	−0.7563
2	0.72	0	0.4578	−0.4639	0.3631	−1.5183
		1	0.6821	−0.5382	0.4218	−1.7941
		2	0.8876	−0.6006	0.4714	−2.0361
	7.0	0	0.5354	−1.0346	0.6419	−6.5882
		1	0.5831	−1.0348	0.6457	−6.5978
		2	0.6303	−1.0351	0.6494	−6.6073

References

[1] Javeri V. Laminar heat transfer in a rectangular channel for the temperature boundary condition of the third kind. Int J Heat Mass Transfer 1978;21:1029–34.
[2] Cuevas S, Ramos E. Heat transfer in an MHD channel flow with boundary conditions of the third kind. Appl Sci Res 1991;48:11–33.
[3] Zanchini E. Effect of viscous dissipation on mixed convection in a vertical channel with boundary conditions of the third kind. Int J Heat Mass Transfer 1998;41:3949–59.
[4] Lukisha AP, Prisnyakov VF. The efficiency of round channels fitted with porous, highly heat-conducting insert in a laminar fluid coolant flow at boundary conditions of the third kind. Int J Heat Mass Transfer 2010;53:2469–76.
[5] Eringen AC. Theory of micropolar fluids. J Math Mech 1966;16:1–18.
[6] Eringen AC. Theory of thermomicrofluids. J Math Anal Appl 1972;38:480–96.
[7] Ariman T, Turk MA, Sylvester ND. Microcontinuum fluid mechanics: a review. Int J Eng Sci 1973;11:905–30.
[8] Ariman T, Turk MA, Sylvester ND. Microcontinuum fluid mechanics: a review. Int J Eng Sci 1974;12:273–93.
[9] Lukaszewicz G. Micropolar fluids: theory and application. Basel: Birkhauser; 1999.
[10] Eringen AC. Microcontinum field theory II: Fluent media. New York: Springer; 2001.
[11] Balaram M, Sastry VUK. Micropolar free convection flow. Int J Heat Mass Transfer 1973;16:437–40.
[12] Agarwal RS, Dhanapal C. Numerical solution of free convection micropolar fluid flow between two parallel porous vertical plates. Int J Eng Sci 1988;26:1247–55.
[13] Chamkha AJ, Grosan T, Pop I. Fully developed free convection of a micropolar fluid in a vertical channel. Int Commun Heat Mass Transfer 2002;29:1021–196.
[14] Cheng CY. Fully developed natural convection heat and mass transfer of a micropolar fluid in a vertical channel with asymmetric wall temperatures and concentrations. Int Commun Heat Mass Transfer 2006;33:627–35.
[15] Prathap kumar J, Umavathi JC, Chamkha AJ, Pop I. Fully-developed free-convective flow of micropolar and viscous fluids in a vertical channel. Appl Math Model 2010;34:1175–86.
[16] Umavathi JC, Sultana J. Mixed convective flow of a micropolar fluid mixture in a vertical channel with boundary conditions of the third kind. J Eng Phys Thermophys 2012;85:895–908.
[17] Rashidi MM, Keimanesh M. Using differential transform method and Pade approximant for solving MHD flow in a laminar liquid film from a horizontal stretching surface. Math Probl Eng 2010;2010:1–14.
[18] Rashidi MM, Mohimanian Pour SA, Hayat T, Obaidat S. Analytic approximate solutions for steady flow over a rotating disk in porous medium with heat transfer by homotopy analysis method. Comput Fluids 2012;54:1–9.
[19] Rashidi MM, Hayat T, Keimanesh M, Yousefian H. A study on heat transfer in a second-grade fluid through a porous medium with the modified differential transform method. Heat Trans – Asian Res 2013;42:31–45.
[20] Prakash D, Muthtamilselvan M, Doh DH. Effect of heat generation on forced convection through a porous saturated duct. Transp Porous Med 2012;95:377–88.
[21] Sheikholeslami M, Hatami M, Ganji DD. Micropolar fluid flow and heat transfer in a permeable channel using analytical method. J Mol Liq 2014;194:30–6.
[22] Srinivasacharya D, Ramana Murthy JV, Venugopalan D. Unsteady stokes flow of micropolar fluid between two parallel porous plates. Int J Eng Sci 2001;39:1557–63.
[23] Bhargara R, Kumar L, Takhar HS. Numerical solution of free convection MHD micropolar fluid flow between two parallel porous vertical plates. Int J Eng Sci 2003;41:123–36.
[24] Zueco J, Eguia P, Lopez-Ochoa LM, Collazo J, Patino D. Unsteady MHD free convection of a micropolar fluid between two parallel porous vertical walls with convection from the ambient. Int Commun Heat Mass Transfer 2009;36:203–9.
[25] Soundalgekar VM. Free convection effects on the stokes problem for an infinite vertical plate. ASME J Heat Transfer 1977;99:499–501.
[26] Abo-Eldahab EM, Ghonaim AF. Radiation effect on heat transfer of a micropolar fluid through a porous medium. Appl Math Comput 2005;169:500–10.
[27] Rahman AM, Sultan T. Radiative heat transfer flow of micropolar fluid with variable heat flux in a porous medium. Nonlinear Anal: Model Contr 2008;13:71–87.
[28] Mohamed RA, Abo-Dahab SM. Influence of chemical reaction and thermal radiation on the heat and mass transfer in MHD micropolar flow over a vertical moving porous plate in a porous medium with heat generation. Int J Therm Sci 2009;48:1–14.
[29] Satya Narayana PV, Venkateswarlu B, Venkataramana S. Effects of hall current and radiation absorption on MHD micropolar fluid in a rotating system. Ain Shams Eng J 2013;4:843–54.
[30] Cogley AC, Vincent WG, Gilles SE. Differential approximation for radiative transfer in a non-gray gas near equilibrium. AIAA J 1968;6:551–3.

D. Prakash received his M.Sc and M.Phil degrees from the Department of Mathematics, Bharathiar University, India in 2009 and 2011, respectively. He is awaiting to get Ph.D degree in Applied Mathematics from Bharathiar University. He is currently working as Senior Research Fellow in the Department of Applied Mathematics, Bharathiar University, India. His research interests are flow and heat transfer in cavities and channel, boundary layer flow and heat transfer analysis of Newtonian and non-Newtonian fluids.

M. Muthtamilselvan received his Ph.D. in 2008 from the Department of Mathematics, Bharathiar University, India. He is currently an Assistant Professor at the Department of Applied Mathematics, Bharathiar University. His research interests are Computational Fluid Dynamics (CFD), convection in nanofluids, boundary layer flow and heat transfer analysis.